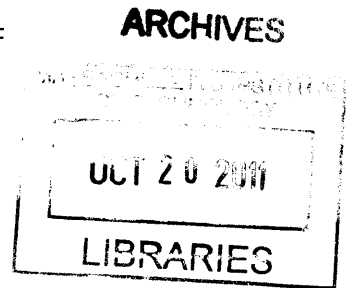# Detecting Sources of Heat Loss in Residential Buildings from Infrared Imaging

by

Emily Chen Shao

SUBMITTED TO THE DEPARTMENT OF MECHANICAL ENGINEERING
IN PARTIAL FULFILLMENT OF THE REQUIREMENTS FOR THE DEGREE OF
BACHELOR OF SCIENCE IN MECHANICAL ENGINEERING
at the
MASSACHUSETTS INSTITUTE OF TECHNOLOGY
June 2011

Signature of Author:____

Emily Chen Shao
Department of Mechanical Engineering
May 6, 2011

Certified by:_____

Sanjay Sarma
Director-MIT-SUTD Collaboration
Thesis Supervisor

Accepted by:_____

John H. Lienhard
Professor of Mechanical Engineering
Chairman, Undergraduate Thesis Committee

Detecting Sources of Heat Loss in Residential Buildings from Infrared Imaging

by

Emily Chen Shao

Submitted to the Department of Mechanical Engineering
on May 6, 2011 in Partial Fulfillment of the
Requirements for the Degree of Bachelor of Science in
Mechanical Engineering

ABSTRACT

Infrared image analysis was conducted to determine the most common sources of heat loss during the winter in residential buildings. 135 houses in the greater Boston and Cambridge area were photographed, stitched, and tallied to characterize nine major causes of heat loss: window frames, window surfaces, window cracks, basements, door cracks, corners, chimneys, roof ridges, and soffits. The nine causes of heat loss were mapped to the three modes of heat transfer: conduction, convection, and radiation.

It was found that heat losses through window surfaces, window cracks, chimneys, and soffits dominated as common sources of energy leakage, each represented in more than 70% of the houses analyzed. Opportunities for future work include more thorough examination of losses through ducts and walls, as well as developing methods for improvements.

Thesis Supervisor: Sanjay Sarma
Title: Director-MIT-SUTD Collaboration

TABLE OF CONTENTS

INTRODUCTION

Energy consumption and efficiency have become issues of growing concern as both supply and demand are strained. In the United States, buildings use 40% of the total energy demanded with more than half of that being consumed by residential buildings as shown in Figure 1. With more than 120 million houses in the United States (US Census Bureau, 2000), this presents a tremendous opportunity to decrease energy consumption and reduce inefficiencies. The purpose of this study is to qualitatively determine common causes of energy loss in residential buildings. This will lead to a better understanding of where to focus attention and resources when it comes to conserving energy in residential buildings.
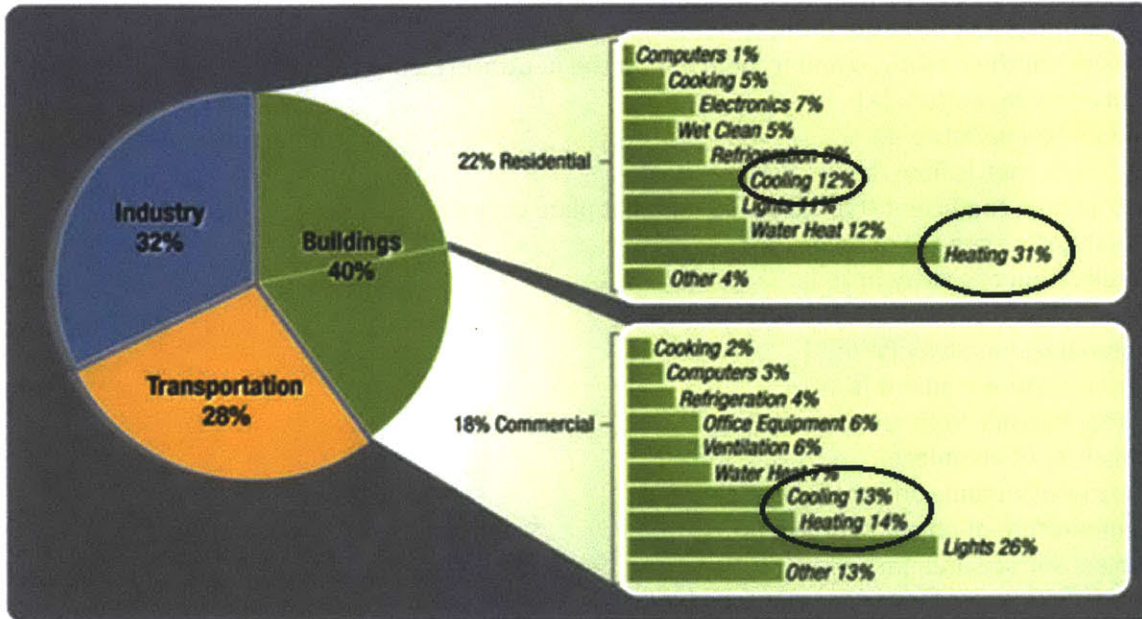

Figure 1: Buildings use about 40% of total US Energy, with residential buildings making up 22% of that energy consumption (Department of Energy)

Figure 1 shows that heating makes up the largest portion of energy consumption in residential buildings. This study focuses on energy lost from heating homes by analyzing infrared images. Current technology allows infrared images to be taken of buildings to show where heat losses occur. A brighter image indicates a hotter area, and a hot area means that there are greater heat losses. The images were taken of houses in the greater Boston and Cambridge area by Long Phan and Jonathan Jesneck of Professor Sanjay Sarma's lab during MIT Thermography Week in January 2010.

The process required capturing high resolution infrared images of hundreds of houses during the month of January, a cold winter month that clearly revealed heat losses in buildings. The high resolution pictures were then stitched together using software to compose complete images. Nine common sources of heat loss were identified and 135 unique images of residential buildings were analyzed. The nine sources of heat loss were mapped back to the basic thermal transfer modes of conduction, convection, and radiation.

It was found that several issues were commonly spotted across the houses, with four issues represented in more than 70% of the residential building analyzed: window surface loss, window crack loss, chimney loss, and soffit loss. The results show that there are many opportunities for improvement in residential buildings, especially in areas that experience severe climates.

LIST OF SYMBOLS

ΔL = change in length [m]

L = initial length [m]

α_L = linear temperature expansion coefficient [m/mK]

ΔT = change in temperature [K]

$\dot{Q}_m$ = heat transfer [J/s]

$\dot{m}$ = mass flow rate [kg/s]

c_p = specific heat [J/kgK]

ΔP = change in pressure [atm]

P_{atm} = atmospheric pressure [atm]

h_o = height of the furthest opening/orifice from the neutral pressure level [m]

T_o = outside temperature [K]

T_i = indoor temperature [K]

Q_{stack} = volumetric flow rate [m^3/s]

C_d = discharge coefficient (typically 0.65 for a flat plate orifice)

A = total surface area of opening [m^2]

g = acceleration of gravity [m/s^2]

q_{cond} = heat flux transfer from conduction [W/m^2]

k = material conductivity [W/mK]

∇T = temperature gradient [K/m]

q_{rad} = heat transfer from radiation [W]

ε = emissivity of an object

σ = Stefan-Boltzmann constant [J/m^{2}K^{4}s]

T_s = temperature of object's surface [K]

A_c = object surface area [m^2]

h_r = radiation heat transfer per unit area [W/m^{2}K]

h_c = conductance [W/m^{2}K]

R_{brick} = thermal conductance of brick [W/mK]

R = thermal resistance [m^{2}K/W]

$\dot{Q}_A$ = heat flux [W/m^2]

BACKGROUND

Heat loss in residential buildings can be traced back to the three basic modes of heat transfer: radiation, conduction, and convection. Models were developed to understand how these types of heat transfer lead to energy losses in buildings.

1. Heat Transfer: Convection

Convection describes the heat transfer through the movement of a fluid. In the case of residential buildings, the air flow in and out of a house results in heat transfer. The two main issues associated with convection are tightness and healthiness of homes. On one hand, from an energy efficiency standpoint, it is desirable to have a tightly constructed house with minimal leakage points and well controlled mechanical ventilation systems. On the other hand, a healthy house needs to breathe in an effective way so that the indoor air has the opportunity to cycle out to release pollutants and allow fresh air inside (Erinjeri, 2009).

Of these two issues, this study will focus on the tightness of homes and how leaks lead to thermal losses. Previous work has been done regarding house tightness, and a standardized format for

measuring air tightness has been developed (Energy Conservatory, 1993). The two measurements that will be referenced are Cubic Feet per Minute at 50 Pascal (CFM50) and Equivalent Leakage Area (EqLA):

CFM50: The airflow (in cubic feet per minute) that needs to be blown through a blower door fan to maintain a pressure differential of 50 Pa between indoors and outdoors.

EqLA: The area of a sharp edged orifice that would leak the same amount of air that the building does at a pressure of 10 Pa.

To develop a basic understanding of the general air tightness of a house in the Boston area, a case study was conducted.

a. Case Study: Determining Crack Size of Boston Back Bay House

The houses in the study are in the greater Boston and Cambridge area, which means that the buildings tend to be older. Therefore, a case study was conducted on a 100-year-old brick house located at 478 Commonwealth Ave in the Back Bay area of Boston.

Figure 2: Front view of the 100-year-old house located at 478 Commonwealth Avenue

To estimate the sizes of cracks in the house, the equation below was used to find the amount of linear change a material will experience under thermal stresses.

$$\frac{\Delta L}{L} = \alpha_L \Delta T \tag{1}$$

It was assumed that the temperature difference between the warm indoors and cooler outdoors was 30 degrees Celsius, or 30 Kelvin. The brick house has about 20 windows and 3 wood doors. The windows were modeled as plate glass with a wood frame, surrounded by brick. The wood and brick were assumed to be joined together with caulk and the cracks were formed at the window and wood interfaces. A schematic is shown below.
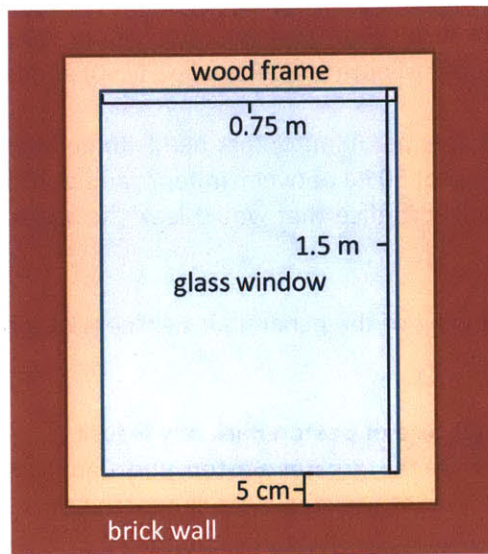
Figure 3: Schematic of an average window in 478 Commonwealth

To apply the linear expansion equation to the model, the temperature expansion coefficients for the various materials needed to be found. They are shown below in Table 1.

Linear Temperature Expansion Coefficient (m/mK)

Plate glass	0.000009
Wood	0.000005
Brick	0.0000055

Table 1: Linear temperature expansion coefficients

Other major sources of air leaks are not as obvious as doors and windows. Leaks in the basement and attic are responsible for most of a home's air leaks. Common attic leaks occur where the walls meet the attic floor and behind or under kneewalls. The basement has many leak areas such as rim joist areas, plumbing vent pipe penetrations, and utility chases. Areas of leakage in other parts of the house include cracks between finish flooring and baseboards, fireplace surroundings, and holes cut for plumbing traps under tubs and showers (Energy Star, 2011). Figure 4 shows the breakdown of sources of air leakages in a house by percentage (US Department of Energy, 2009).
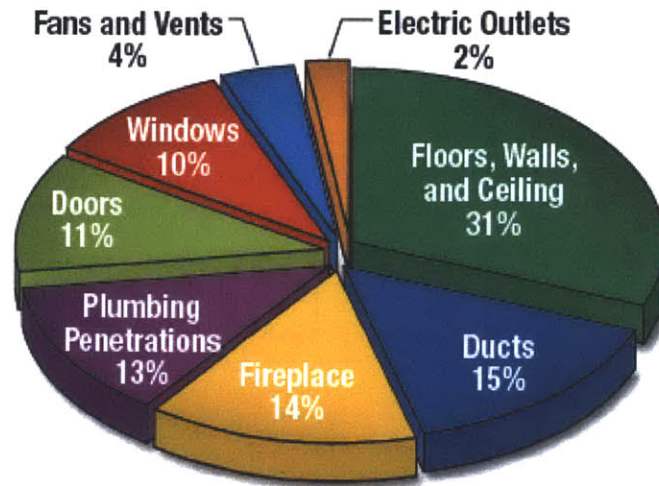
Figure 4: Sources of air leakages in a house as a percentage of total leakage

The total surface area of the cracks and leaks at the joints of doors and windows was found to be about 0.05 m^2 (detailed calculations in Appendix A: Case study leakage calculation). Considering windows and doors as approximately 20% of the total leak area, the total leak area of the house was found to be about 0.26 m^2. This is significant because it means that if all the cracks and leakage points in the house were consolidated into one orifice, it would be equivalent to a hole in the side of the house with a surface area of 0.26 m^2.

b. Blower Door Test

The blower door test is a diagnostic tool used by builders to quantify the leakiness of a house (Van der Meer). The process begins by installing a variable speed fan in a door frame with an adjustable, sealed door panel. While in operation, the blower door fan serves as an exhaust fan and vents indoor air to the outside. This process sucks air out of the house and causes the air pressure in the house to drop below the pressure of the air outside. The pressure differences tested range anywhere between 10 to 60 Pa, although the results are standardized to a difference of 50 Pa (using the standard of cfm50). The ranges of cfm50 are shown in the table below.

House Leakiness Category	cfm50
Tight House	<1,200
Moderately Leaky House	1,200-3,000
Very Leaky House	>3,000

Table 2: Relationship between cfm50 and leakiness of a house (Van der Meer)

Equipped with a house's cfm50, one can approximate the equivalent leakage area (EqLA). The correlation between cfm50 and the EqLA in inches squared is about 0.1 (Erinjeri, 2009), meaning that a house with a cfm50 of 1200 would have an EqLA of about 120 inches squared.

Considering that the houses in Kenmore Square are more than 100 years old, it is expected that the buildings will be extremely leaky because the building materials have undergone decades of wear (Chan, 2005). Therefore, it can be hypothesized that an old house would have a cfm50 of at least 3,000. If a

cfm50 of 4,000 were used to be conservative, it would result in an EqLA of about 0.25 m^2, which is quite close to the leakage calculation of 0.26 m^2 in the previous section.

Equipped with a sense of the size of the cracks in a house, the next step is to determine the mass air flow through these cracks. Figure 5 shows how air mass flow through cracks of a building can result in heat transfer. When there is a temperature difference at the two ends of the mass air flow, such as in a building when it is warmer indoors in the winter compared to the outdoors, heat transfer is dependent on both the amount of mass flow as well as the difference in temperature, as highlighted in equation 2.
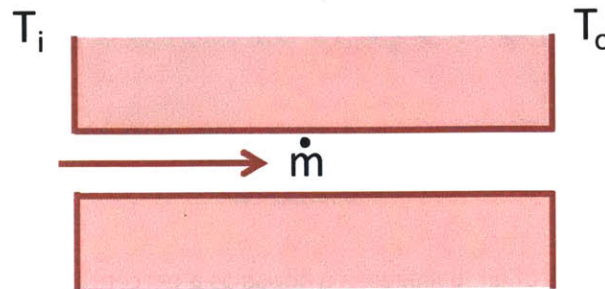
Figure 5: Mass flow through a crack results in heat transfer

$$\dot{Q}_m = \dot{m} c_p \Delta T \tag{2}$$

Air is moved in and out of a house by three main forces: the stack effect, mechanical systems, and wind (Harley, 2002). The stack effect is constant and driven by buoyancy. A greater thermal difference results in more air flow, so this effect is highly prevalent in more severe climates. Wind contributes to drafts and airflow as well, but because it is an irregular occurrence compared to the stack effect, it has a relatively smaller impact on total air flow (Harley, 2002). Finally, mechanical systems such as fans, air handlers, combustion appliances, and ducts also move air through houses. However, each house's mechanical systems are unique and push air around in unpredictable ways. For this study, the focus will be on the stack effect.

c. The Stack Effect

Air flow due the stack effect is caused by pressure differences and air buoyancy in the building. During the winter months, cold air tends to seep into the house from the lower levels, and then heated air escapes the building from the top. This is known as the stack effect. Because warmer air is lighter and more buoyant, a higher pressure results at the top of the house. The higher pressure at the top of the building creates a pressure differential, with the higher pressure warm air escaping the building to achieve a pressure balance. Meanwhile, the bottom of the house experiences a negative pressure where the pressure inside is lower than the pressure outside. This causes the cold air to seep in through the cracks. The effect is illustrated in Figure 6. It should be noted that there is a certain height in the building where the pressure of the air indoors matches the pressure of the air outdoors. This height is known as the neutral pressure level.
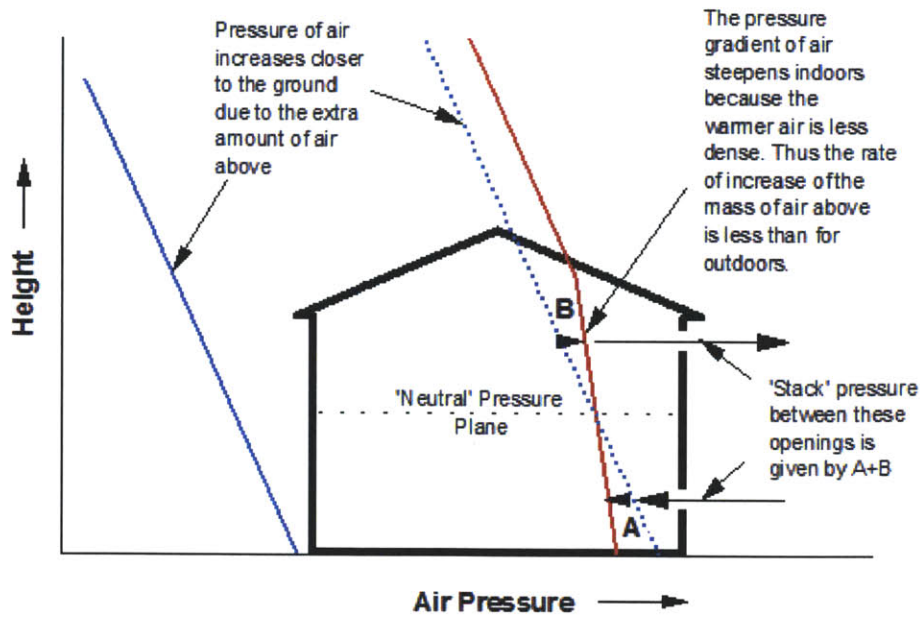
Figure 6: Illustration of the stack effect in a house (Veetech, 2010)

A sampling of infrared images of residential buildings is illustrative of the stack effect. Many images show bright spots near the rooftops and peaks of the houses, as shown in Figure 7 below. This is indicative of warmer, higher pressure air leaking out of the cracks at higher elevations.
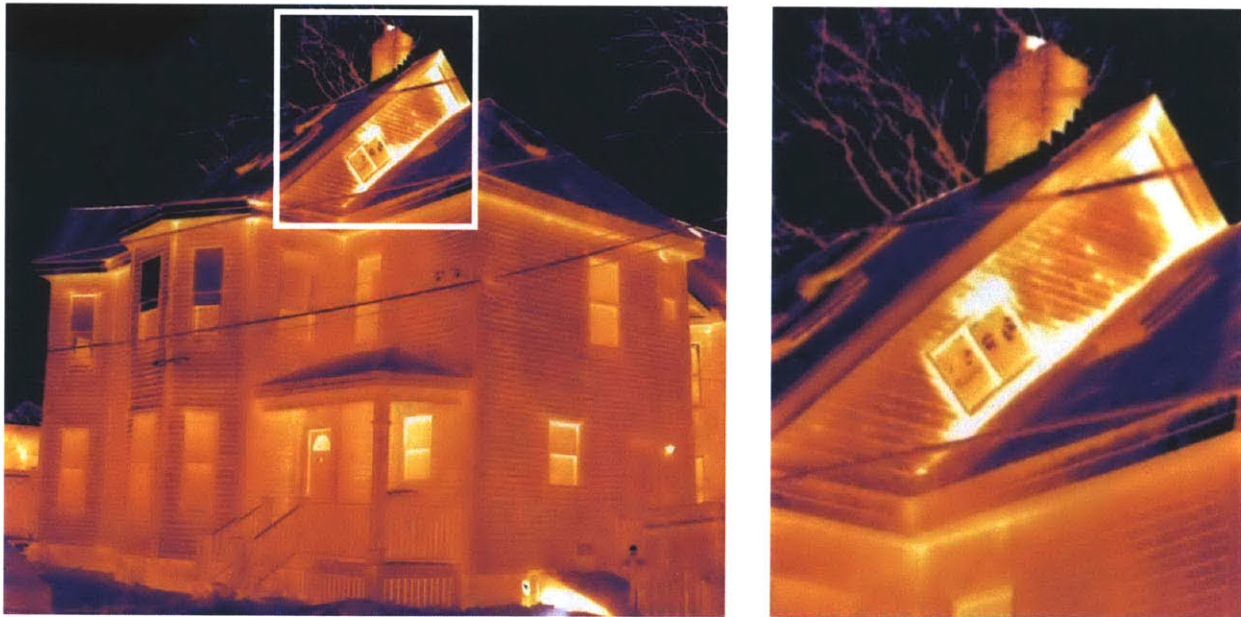

Figure 7: Infrared image of a residential building and a close-up of the roof to highlight heat losses

When conducting the case study on 478 Commonwealth, different areas of potential air leakage in the house were qualitatively assessed to better understand the stack effect and how air cycles through a building. Besides using one's hands at the leakage areas to feel the direction of air flow, a simple tool

was constructed using a skewer and dark colored threads, shown in Figure 8. This allows for a pictorial understanding of air flow.

Figure 8: Thread tool constructed to identify air flow direction in 478 Commonwealth

The first area of investigation was the basement. The basement is the lowest accessible part of the house. Because the pressure of the colder air is greater at this level, it is expected that the cold air will flow into the house. This was affirmed when placing one's hands by the basement door cracks, and can be seen in Figure 9.

Figure 9: The lowest accessible point of 478 Commonwealth was the basement. The highlighted circle is where the air flow was tested. The direction of the threads shows that air was blowing into the house.

The next area analyzed was a window on the fourth floor of the building, the highest floor. Lighter, more buoyant warm air travels up to higher levels and results in a higher pressure compared to the air outside. When using one's hand to test air flow, there was a feeling of suction, which results from the warmer air flowing out of the house because of its relatively higher pressure. This was also indicated by testing with the thread tool.
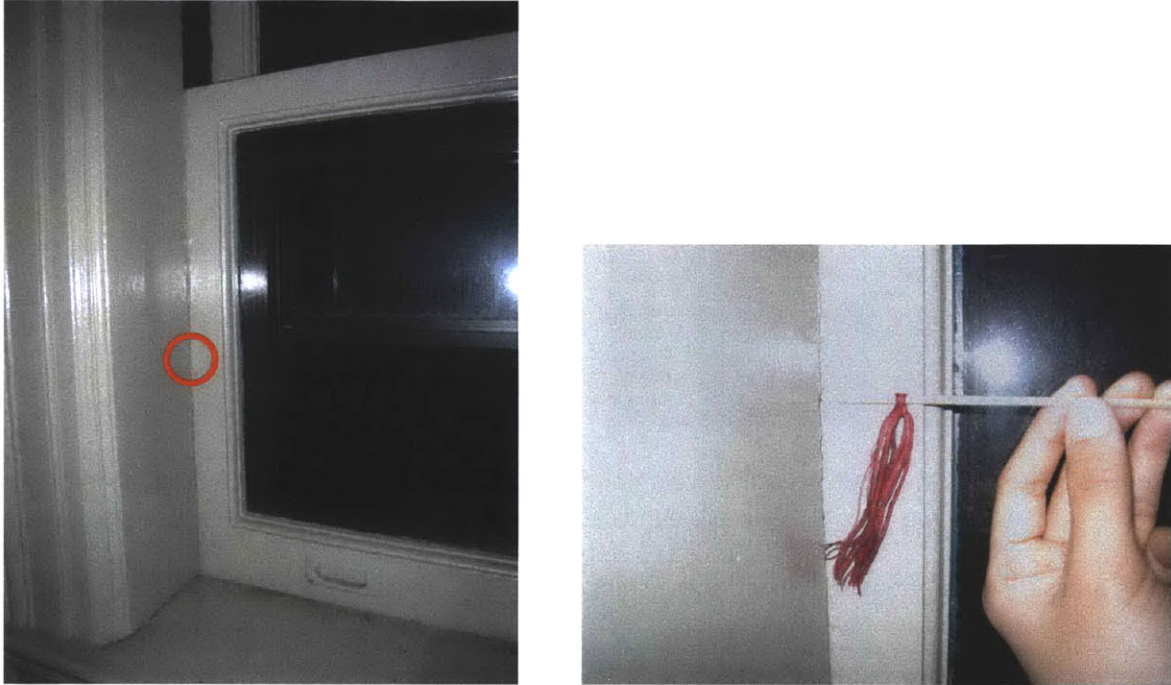
Figure 10: The highest accessible point of 478 Commonwealth was the fourth floor. When placing the thread tool at the window crack, the threads were drawn towards the crack, indicating that the warm indoor air was escaping.

Finally, the large windows on the second floor of the building were tested to identify the neutral pressure plane. This is the height where the indoor air pressure matches the outdoor air pressure, and although there may be cracks, the stack effect states that the balance of pressures results in zero air flow. Using the thread tool, it was shown that the neutral pressure plane of 478 Commonwealth is located on the second floor, as shown in Figure 11.

Figure 11: The large windows on the second floor of 478 Commonwealth had substantial cracks, but when the thread tool was used there was no indication of air flow because of the neutral pressure plane.

The pressure differential as a result of the stack effect is found using Equation 3 (Walker, 2010).

$$\Delta P = 0.342 P_{atm} h_o \left(\frac{1}{T_o} - \frac{1}{T_i} \right)$$

(3)

Equipped with this information, the volumetric flow rate from given cracks can be determined from the equation below (Walker, 2010). To determine the mass flow rate out of the cracks due to the stack effect, multiply the Q_{stack} found by the air density.

$$Q_{stack} = C_d A \sqrt{2gh_o \left(\frac{T_i - T_o}{T_i} \right)}$$

(4)

2. Heat Transfer: Radiation and Conduction

The other types of heat loss to be considered are conduction and radiation. Conductive heat loss is due to movement of heat through solid materials and is dependent on the materials' thermal conductivity. The better insulated and less thermally conductive a material is the less heat will be lost through it. Specifically, heat loss from conduction can be found using the equation below.

$$q_{cond} = -k\nabla T$$

(5)

Radiation is the heat transfer from one object to another through space. The amount of heat loss is dependent on the temperature differences of the two surfaces in of interest. Heat losses caused by radiation only happen when there is a direct line of sight between two objects that have different

temperatures (Harley, 2002). The equation below shows the simplistic Stefan-Boltzmann's equation for radiation heat loss.

$$q_{rad} = \varepsilon\sigma\left(T_s{}^4 - T_o{}^4\right)A_c \qquad (6)$$

This equation shows that the greater the difference between the temperatures, the more heat is lost through radiation. As can be seen in the equation, a material's emissivity also impacts the radiation. Some common materials' emissivity values are shown in Table 3.

Material	Emissivity (ε)
Glass	0.80-0.95
Brick	0.93
Cement	0.54
Concrete	0.92-0.97
Aluminum-oxidized	0.11-0.31
Iron-oxidized	0.94
Stainless steel-oxidized	0.74-0.87

Table 3: Emissivity values of common materials

The application of Planck's law leads to a simplified version of Stefan-Boltzmann's equation, which provides the per unit area radiation heat transfer.

$$h_r = \varepsilon\sigma T_m{}^3 \qquad (7)$$

$$T_m = \frac{T_s + T_o}{2} \qquad (8)$$

As shown in the equation above and the figure below, heat transfer due to radiation is a cubic function of the mean temperature of the surface in question and its surroundings. This non-linear relationship shows that the higher the temperature difference, the greater the heat transfer.
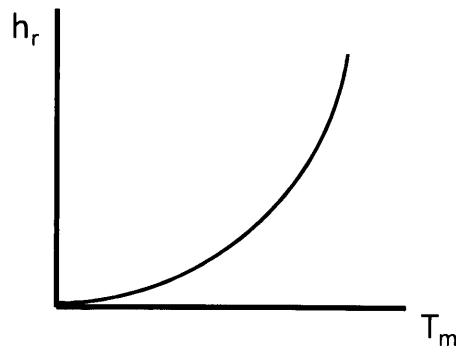
Figure 12: Cubic relationship between radiation heat transfer and mean temperature of surface of interest and its surroundings

Combining the effects of radiation and conduction, the figure below illustrates a schematic of the heat losses from a cross section of a brick wall.
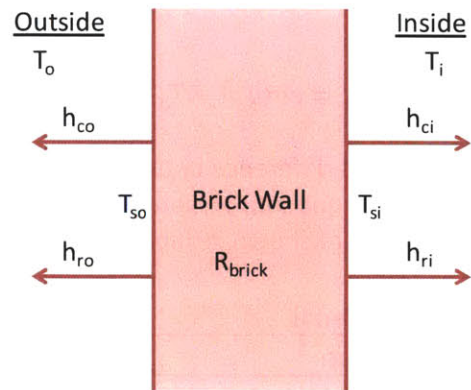
Figure 13: Schematic of radiation and conduction heat losses across a brick wall

Thermodynamic theory allows conduction and radiation losses to be modeled as a circuit diagram, as shown below. The heat "resistances" can be added in series and parallel, similar to a circuit, to determine the equivalent heat "resistance".
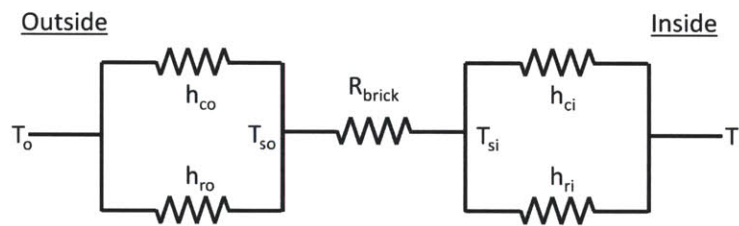
Figure 14: Equivalent radiation and conduction heat transfer circuit diagram

3. Determining Total Energy Lost

With a basic understanding of heat transfer, it is possible to determine a residential building's total energy loss over the course of a year. The first step is to determine the overall thermal resistance of the house, which is known in industry as the R value (the ratio of the temperature difference across a material and the heat flux). Because heat flux is a measurement of heat energy transfer through a given surface, it is determined by the house's thermal conductivity and radiation heat transfer coefficients.

$$R = \frac{\Delta T}{\dot{Q}_A} \tag{9}$$

The table below shows R values for common materials used in house construction. Although the table lists values in SI units, it is very common in the United States to use units of $ft^2 hr°F/BTU$.

R value for inch thick material [m^{2}K/W]

Vacuum Insulated Panel	5.28-8.8
Silica Aerogel	1.76
Polyurethane Rigid Panel	1.20
Urea Foam	0.92
Polystyrene Board	0.88
Home Foam	0.69
Wood Fill	0.18
Brick	0.03
Glass	0.025
Poured Concrete	0.014

Table 4: R values for common home construction materials of one inch thickness

With a given R value for a house, the total energy loss over a day can be found, given the surface area of interest and the temperature difference between indoors and outdoors. It is important to note that different sections of a house will have different R values. For example, the walls of a brick building will have a given R value, but the basement may have a lower R value because it is made of concrete. Likewise, the ceiling will also have a different R value because different materials were used to construct that part of the house.

$$Heat\ loss\ per\ day = \frac{A_c \Delta T}{R}(24\ hours) \tag{10}$$

Besides determining the amount of energy loss on a given day, energy loss can also be quantified for an entire year. The first step is to calculate the energy loss per degree day, which is the amount of energy lost over one day given that there is one degree temperature difference between the indoors and outdoors.

$$Loss\ per\ degree\ day = \frac{A_c(1K)}{R}(24\ hours) \tag{11}$$

Given a house's energy loss per degree day, the final piece of data needed is the quantity of degree-days over a year for a house, or average temperature difference multiplied by the number of days in home's heating season. This is something that can be measured and will depend on the climate and location of the house.

$$Annual\ heating\ energy\ loss = (loss\ per\ degree\ day)(degree\ days) \tag{12}$$

PROCEDURE

To understand the major sources of heat loss in residential buildings, infrared images were taken of hundreds of houses in the greater Boston and Cambridge area. The images were taken at night throughout the month of January 2010, one of the coldest months of the year, so that areas of heat loss would be clearly highlighted. The camera used was an infrared FLIR P660 (see Appendix B: FLIR P660 camera specifications). The camera had a low resolution of 640 x 480 per picture. However, the analysis required specific features of the houses to be clearly seen. To correct for the low resolution, focused

images of segments of the houses were taken. A software (PTGui) was used to stitch the segmented images together.

Figure 15: Screenshot of PTGui being used to stitch segmented images into a panorama
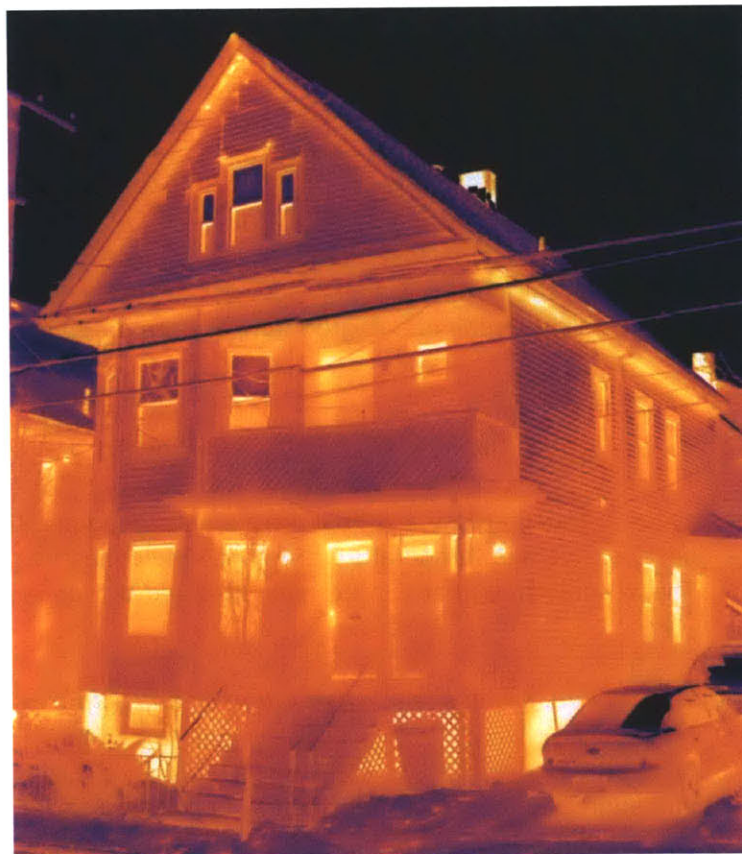
Figure 16: Complete panorama stitched from segmented images

A total of 135 complete panoramas were stitched together. The next step was to review the panoramas and identify the main sources of heat loss. The major types of heat loss are described below.

Window frame and casing loss: Heat loss can occur at the casing and frame of the windows if the spaces have not been properly sealed. Casings that are not tight allow for a lot of air to leak through, resulting in heat loss due to convection and air mass flow. When installing windows, these gaps should be sealed using caulk (Harley, 2002).
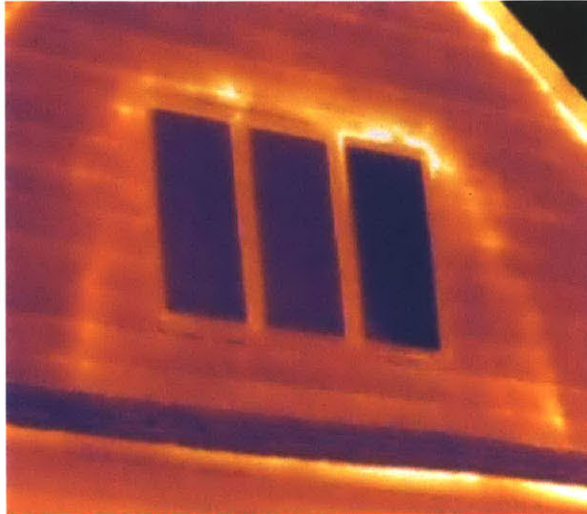
Figure 17: Infrared image of window frame and casing loss

Window surface loss: Glass windows are common sources of heat loss because of conduction, airflow by the glass, as well as radiation (dependent on the emissivity of the glass). Several standards are used to measure energy efficiency of windows. The U-factor represents the conductive heat loss, where the smaller the value the less conductive, which means less heat loss (NFRC, 2005). The solar heat gain coefficient (SHGC) measures the amount of direct solar radiant heat that enters through a window. A higher SHGC value increases solar heat gains in the winter (Harley, 2002).
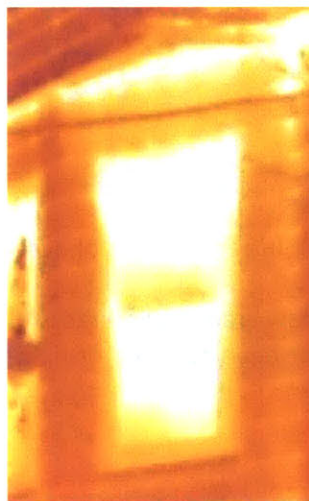
Figure 18: Infrared image of window surface loss

Window crack loss: Older buildings have experienced decades of harsh winters and hot summers. The extreme temperatures have expanded and contracted the building materials for years, resulting in weaker materials. This creates cracks in areas around the perimeter of windows where the frame and glass join together. These cracks allow for heat to be lost due to air mass flow, or what is commonly known as a draft.
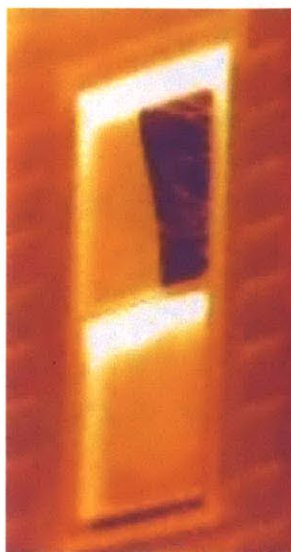
Figure 19: Infrared image of window crack loss

Basement loss: Conductive and radiation heat losses result from poorly or un-insulated basements (Yost, 2002). Air leakage can also occur along the top of the basement wall where the cement contacts the wood frame (Energy Star, 2000).The perimeter framing (rim joist) creates cavities along the basement wall that allows for leakage to occur.

Figure 20: Infrared image of basement loss

Door crack loss: Similar to the window crack leaks, cracks form around doors that have experienced many years of weather and have not been repaired or tightened. These cracks lead to air mass flow and convective heat loss.

Figure 21: Infrared image of door crack loss

Corner loss: Heat loss can occur at the corners of walls when a gap is created in the thermal boundary. This can be caused by either a discontinuous air barrier or poor insulatio. When two walls come together to form a corner, the joining point may not be as tight, resulting in a gap.
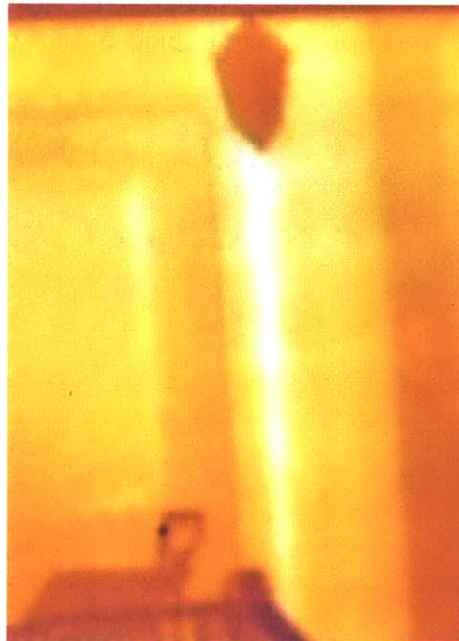
Figure 22: Infrared image of corner loss

Chimney loss: A chimney that protrudes above the ceiling has a higher neutral pressure zone than the rest of the house. Combined with the stack effect, this results in a flow of air into the fireplace and out of the chimney, even if there is no fire burning. Although dampers are installed to seal the chimney flue when not in use, many dampers do not close tightly and could even be installed incorrectly. Heat losses due to air mass flow could be significant depending on the leakage area.

Figure 23: Infrared image of chimney loss

Roof ridge loss: Because of the stack effect, warm air travels up toward the attic in a house. If there are gaps in the thermal boundary around the roof ridge area, heat loss will occur due to warmer air flowing out (stack effect), and conduction with the colder outside surface.
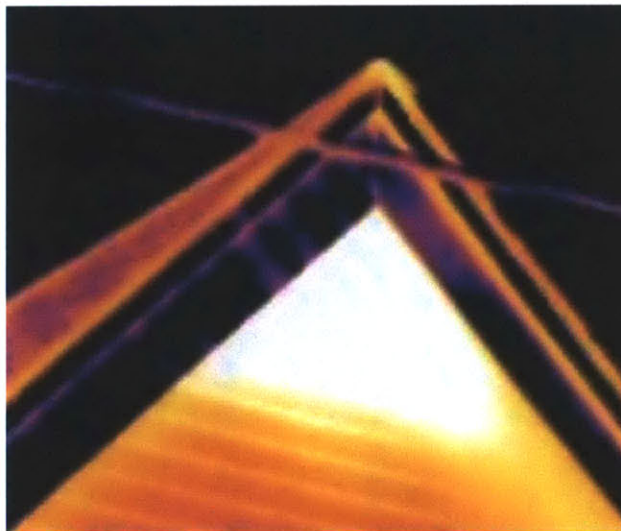
Figure 24: Infrared image of roof ridge loss

Soffit loss: Heat loss can occur near the soffits if the area around the joists are not properly insulated or sealed. Because the soffits are located higher up on the house, gaps allow for convection (air mass flow), while poor insulation results in losses due to conduction.

Figure 25: Infrared image of soffit loss

After the main sources of heat loss were identified, each image was analyzed to determine which problem areas occurred in each house. Each house's problem areas were documented (see Appendix C: Table of residential building mapping for sources of heat loss) and a tally was kept, along with the relevant segments of the image. If a house had multiple occurrences of the same problem area, such as several windows that had significant surface loss, the problem area was only counted once. This is because the purpose of the tally was to develop an understanding of the number of houses that have a certain heat loss issue, as opposed to the total number of problem areas that occurred.

RESULTS AND DISCUSSION

Tallying the nine major problem areas for 135 images of residential buildings resulted in a clearer understanding of what heat loss issues are most common in residential buildings. (see specific images in Appendix C: Table of residential building mapping for sources of heat loss)
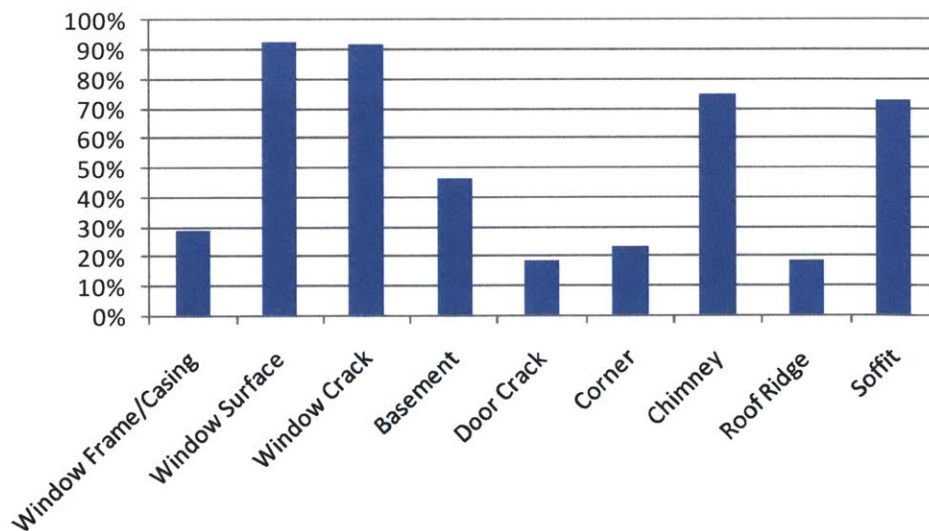
Figure 26: Percentages of major sources of heat loss for 135 houses

The results show that the most common problems are related to windows, whether it is heat loss due to conduction through window surfaces, or air leaking out of the cracks of the window edges. This is

23

because many of the older houses in the New England area use single-pane windows. These windows do not insulate well, and the older frames have survived years of weathering which lead to cracks and leaks.

Over the past few decades, window technology has improved to offer consumers high-efficiency windows that feature double panes. From a conduction standpoint, these windows include low emissivity and solar control coatings, as well as low conductance gas fills such as argon or krypton. To minimize leakage of hot air through cracks, the windows are installed with improved thermal breaks, edge spacers, and better edge sealing techniques (Energy Star, 2000). Some window installations also use different window frames. For example, a fiberglass frame is not only more dimensionally stable than vinyl and wooden frames over time, it also conducts less heat than its older predecessors.

New frame materials
and designs

Low-emissivity and/or
solar control coatings

Low conductance gas fills

Insulating spacer
between glazings
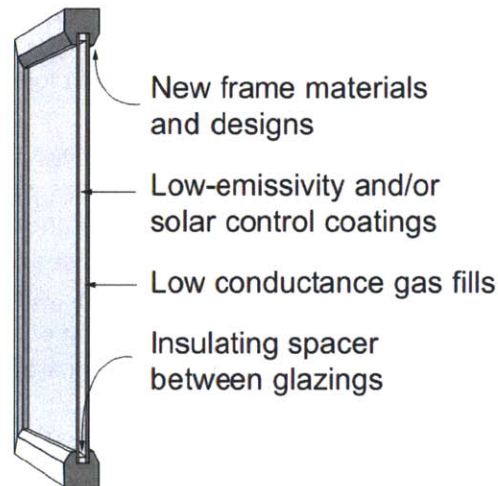
Figure 27: Higher thermal efficiency window that is becoming more common (Energy Star, 2000)

While analyzing images of residential buildings, it was evident that some houses had changed their less thermally efficient single pane windows for more efficient ones. When counting the number of houses that had at least one well-insulated window, the overall percentage was 82%, although for most homes, the majority of windows were poorly insulated.
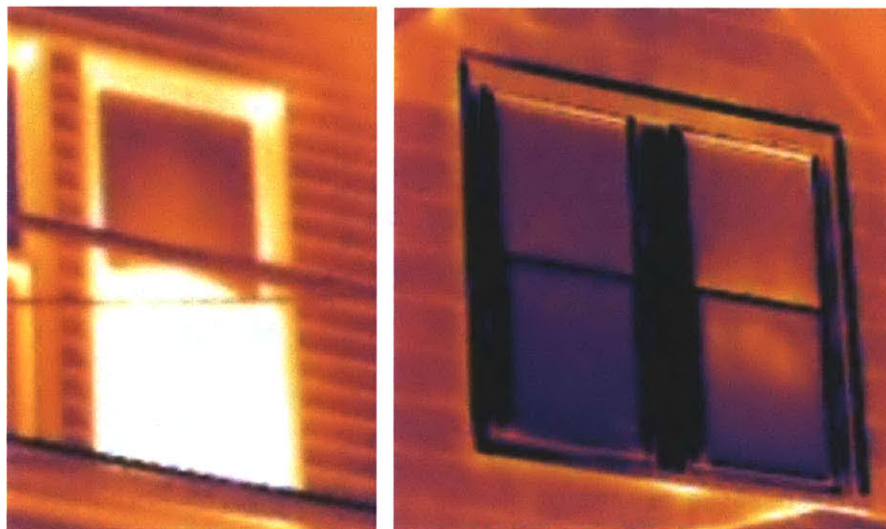
Figure 28: Infrared images contrasting highly conductive windows and more thermally efficient windows

Although many older houses experience heat loss through poorly insulated windows, it does not necessarily mean that the best solution is to replace all windows. Although a highly prevalent issue, heat loss through windows represents less than 20% of a typical New England house's heating bill, as shown in Figure 29 (Harley, 2002). If highly efficient windows are purchased at a low price and self installed, the payback period is on the range of 20 years, a payback period that may be too long for homeowners who do not plan to stay in the same house for such an extended time. This introduces the dilemma of a homeowner's personal financial interests and how to balance that with a reduction in energy consumption and an increase in efficiency. Other ways to decrease energy loss through windows is to make adjustments to the current windows, whether it is adding a storm sash, or caulking and sealing the edges of the frame.
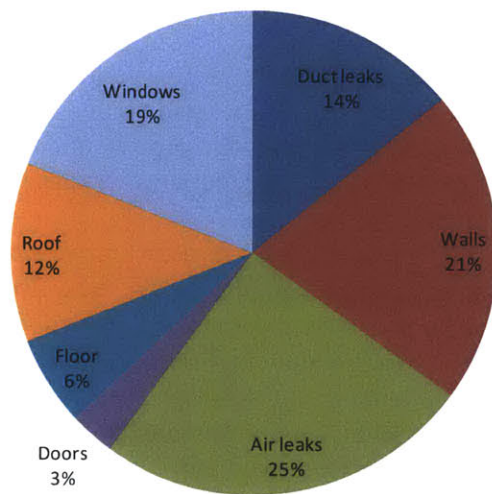
Figure 29: Distribution of annual heating bill losses for a typical New England house (Harley, 2002)

If a homeowner chooses to replace their windows, not only is it important that the new windows are thermally efficient, but also that the installation process is executed carefully. As shown in the data in Figure 26, nearly 30% of houses experience heat losses at the window casing and frame.

Another high count problem area is the chimney, with about 75% of all houses with chimneys experiencing heat loss through the chimney. Because a chimney is designed specifically for smoke to escape, a fireplace with a flue damper that is not tightly closed will allow air to escape every hour of the day. In addition, a chimney leads to the top of the building and is often the highest point. With an open damper, the heat losses from the stack effect are exacerbated because of the geometry and position of the long, tall chimney. If a house has a fireplace but does not use it, energy can be conserved by plugging and sealing the chimney flue. One of the best ways to minimize heat loss through a chimney is to examine the flue damper, since the dampers may not close tightly or may be warped after exposure to the heat from the fireplace (US Department of Energy, 2009).

Many houses experience heat losses along the soffits as well, at the underside of roofs where the walls join the ceiling, with just over 70% of houses experiencing this type of heat loss. These thermal losses result from air mass flow through the leaks that develop over years of weathering. A common fix to these issues is to improve insulation and to reseal areas around the joists.

Heat loss through basements was identified in nearly 50% of the houses, and infrared images showed that the regions of heat loss were very bright and had a large surface area. Although not as prevalent an issue as the ones previously described, heat loss from an uninsulated basement could

account for up to one third of the heating costs in an average home (Timusk, 1981). Depending on the use of the basement, a homeowner may choose not to insulate the basement area. There are three ways to insulate a basement wall: in the middle, on the interior, or on the exterior. The most common approach has been to insulate the interior because of cost reasons. However, proper insulation installation is dependent on the controllability of moisture flow and airflow. If these factors are not controlled well, additional insulation could result in material deterioration, mold growth, and dangerous indoor air quality.

Although a specific count was not made for thermal losses through the walls or ceilings, the infrared images clearly showed that a large portion of a house's heat loss can be attributed to radiation and conduction losses through the wall and ceiling surfaces. Both Figure 4 and Figure 29 indicate that walls result in 31% of the thermal losses and account for 21% of the costs lost. These losses are a function of the materials used for both wall construction and insulation.

CONCLUSIONS

As energy supply and demand issues become more prevalent, it is important to not just find ways to generate a greater supply, but to also tackle the demand side. This study takes the first step with residential buildings in the great Boston and Cambridge area by qualifying the main problem areas that lead to heat loss. It was found that many houses experience similar issues, with windows, soffits, and chimneys being common problem areas for heat loss.

Of the different modes of heat transfer, air leaks through cracks and ducts account for nearly 40% of the energy lost when heating a residential building, while conduction through walls and windows account for the other 40% of energy lost. This provides a simplified framework for determining where resources and technology should be focused on when reducing energy loss in homes. The priorities of homeowners should be on sealing air leaks to cut down on air mass flow in and out of the house, while building developers should focus their attention on constructing homes with higher R values so that less heat is lost through windows and walls due to conduction.

Equipped with a better understanding of the main types of heat loss and where they generally occur, engineers, building developers and homeowners will be able to better identify sources of heat losses in residential buildings and fix the problems to reduce energy waste. There are also many opportunities to further develop this work, such as developing methods to reduce the most common sources of heat loss, and expanding from residential buildings to commercial infrastructure. Moving forward, it will also be useful to evaluate heat loss issues that are not as visible through infrared images, such as heat losses through duct leaks and plumbing penetrations.

REFERENCES

Chan, W., Nazaroff, W., Price, P., Sohn, M., Gadgil, A., 2005. Analyzing a database of residential air leakage in the United States. Science Direct. Atmospheric Environment 39.

The Energy Conservatory, 1993. Minneapolis Blower Door Operation Manual, Minneapolis, MN.

Energy Star, 2000. High-Performance Windows. US Environmental Protection Agency.

Energy Star, 2011. Locating Air Leaks. US Department of Energy & US Environmental Protection Agency.

Erinjeri, J., 2009. Empirical Modeling of Air Tightness in Residential Homes in North Louisiana. Louisiana Tech University.

Harley, B., 2002. Build Like a Pro: Insulate and Weatherize. The Taunton Press, Newtown, CT.

NFRC, 2005. The Facts about Windows and Heat Loss. National Fenestration Rating Council.

Timusk, J., 1981. Insulation Retrofit of Masonry Basements. Department of Civil Engineering University of Toronto, for the Ontario Ministry of Housing.

US Census Bureau, 2000. Census of Housing: Historical Census of Housing Tables.

US Department of Energy, 2009. Energy Savers Booklet: Tips on Saving Energy and Money at Home. Office of Energy Efficiency and Renewable Energy.

Van der Meer, B. Blower Door Testing. The Pennsylvania Housing Research Center.

Veetech, 2010. The Driving Forces for Natural Ventilation. Ventilation Energy and Environmental Technology.

Walker, A., 2010. Natural Ventilation. Whole Building Design Guide: A Program of the National Institute of Building Sciences.

Yost, N., Lstiburek, J., 2002. Basement Insulation Systems. Building Science Corporation.

APPENDIX A: CASE STUDY LEAKAGE CALCULATION

Assumptions		Constants	
Temperature Diff (ΔT) [K]	30	α_L Plate glass [m/mK]	0.000009
Number of Windows	20	α_L Wood [m/mK]	0.000005
Number of Doors	3	α_L Brick [m/mK]	0.0000055
Glass Window Width (w_w) [m]	0.75		
Glass Window Height (w_h) [m]	1.5		
Wood Frame Width (f_w) [m]	0.05		
Brick Frame Width (f_b)[m]	2		
Door Width (d_w) [m]	0.91		
Door height (d_h) [m]	2.1		
% Leak from Windows & Doors	20%		

Window Crack Size Calculations

	Equation	Value
% Glass Shrink ($\%_g$)	$\Delta T \times \alpha_L$	0.027%
% Wood Shrink ($\%_w$)	$\Delta T \times \alpha_L$	0.015%
% Brick Shrink ($\%_b$)	$\Delta T \times \alpha_L$	0.017%
Glass Horizontal Crack [m^2]	$\%_g \times w_w \times w_h$	0.00030
Glass Vertical Crack [m^2]	$\%_g \times w_w \times w_h$	0.00030
Wood Horizontal Crack [m^2]	$\%_w \times w_w \times f_w$	0.00001
Wood Vertical Crack [m^2]	$\%_w \times w_h \times f_w$	0.00002
Brick Horizontal Crack [m^2]	$2 \times \%_b \times f_b \times (w_w + 2 \times f_w)$	0.00056
Brick Vertical Crack [m^2]	$2 \times \%_b \times f_b \times (w_h + 2 \times f_w)$	0.00106
Total one Window Crack [m^2]	Σwindow cracks	0.00226
Total Window Crack (c_w) [m^2]	20 x Σwindow cracks	**0.04517**

Door Crack Size Calculations

	Equation	Value
Wood Horizontal Crack [m^2]	$\%_w \times d_w \times d_h$	0.00029
Wood Vertical Crack [m^2]	$\%_w \times d_w \times d_h$	0.00029
Brick Horizontal Crack [m^2]	$\%_b \times d_w \times f_b$	0.00030
Brick Vertical Crack [m^2]	$2 \times \%_b \times d_h \times f_b$	0.00139
Total one Door Crack [m^2]	Σdoor cracks	0.00226
Total Door Crack (c_d) [m^2]	3 x Σdoor cracks	**0.00678**

Total Crack Size Calculations

	Equation	Value
Total Crack Size (c_T) [m^2]	$c_w + c_d$	0.05
Total Leakage Area [m^2]	$(c_T)/20\%$	**0.26**

FLIR P Series

FLIR P660
The High Performance infrared inspection system

FLIR P660 is the highest performing infrared inspection system available. With its state of the art technology, including 640x480 detector resolution and unique ergonomic design it is the natural choice for professional thermographers that want the most efficient instrument producing professional results. There are three standard set available for option:

1. The camera is equipped with standard 24° lens.
2. The camera is equipped with a 12° telephoto lens with 2x higher magnification
3. The camera is equipped with a 45° wide angle lens particularly useful when studying large areas at close distance.

- *Image resolution 640x480*
- *Sensitivity 30 mK*
- *Large high resolution 5.6" flip-out LCD*
- *Tiltable high resolution viewfinder*
- *High performance lenses with USM technology*
- *1-8 times continuous zoom with pan*
- *Contrast optimization*
- *Rotatable handle for convenient operation*
- *Built-in 3.2 Mpixel digital camera with target illuminator*

- *Standard temperature range -40 °C to 500 °C*
- *1%, 1°C accuracy*
- *Real time radiometric storage to built-in RAM*
- *Periodic storage*
- *Panorama*
- *Voice and text annotation*
- *Built-in GPS*
- *MPEG-4 streaming to PC using USB or FireWire*
- *Programmable buttons*

GPS technology helps to record location information

FLIR Systems FLIR P660 is an affordable easy-to-operate high-performance infrared camera that delivers accurate temperature measurements at productive and safe distances. This makes the P660 camera an ideal solution for cost-effective and efficient predictive maintenance programs.

The P660 includes an integrated 3.2 megapixel camera to aid in reporting. Infrared and visual images taken with the P660 can be stored in standard JPEG formats. The P660 visual camera includes matching Field Of View lenses, so IR and visual images are shown at similar long distances using the same Field Of View.

Fusion, a function that lets you display a part of digital photo as an infrared image.

Infrared inspection helps to detect overheating parts, can avoid costly downtime and maintain plant efficiencies.

29

FLIR P660 Technical Specifications

Imaging and optical data	
Field of view (FOV) / Minimum focus distance	12° × 9° / 1.2 m
Spatial resolution (IFOV)	0.33 mrad
Thermal sensitivity / NETD	30 mK @ +30°C
Image frequency	30 Hz
Focus	Automatic or manual (electric or on the lens)
Zoom	1–8× continuous, digital zoom, including panning
Focal Plane Array (FPA) / Spectral range	Uncooled microbolometer / 7.5–13 μm
IR resolution	640 × 480 pixels
Image presentation	
Display	Built-in widescreen, 5.6 in. LCD, 1024 × 600 pixels
Viewfinder	Built-in, tiltable LCD, 800 × 600 pixels
Automatic image adjustment	Continuous / manual; linear or histogram based
Manual image adjustment	Level/span / max / min
Contrast optimization	Automatic, adjustable DDE
Image modes	IR-image, visual image, thumbnail gallery
Reference image	Shown together with live IR image
Measurement	
Temperature range	−40°C to +500°C
Accuracy	±1°C or ±1% of reading for limited temperature range, ±2°C or ±2% of reading
Measurement analysis	
Spotmeter	10
Area	5 boxes or circles with max. / min. / average
Automatic hot / cold detection	Max / Min temp. value and position shown within box, circle or on a line
Isotherm	2 with above / below / interval
Profile	1 live line (horizontal or vertical)
Difference temperature	Delta temperature between measurement functions or reference temperature
Reference temperature	Manually set or captured from any measurement function
Emissivity correction	Variable from 0.01 to 1.0 or selected from editable materials list
Measurement corrections	Reflected temperature, optics transmission, atmospheric transmission and external optics
Measurement function alarm	Audible/visual alarms (above / below) on any selected measurement function
Set-up	
Set-up commands	Configurable measurement tools menu; configure information to be shown in image; 2 Programmable buttons; user profiles; local adaptation of units, language, date and time formats
Storage of images	
Image storage	Standard JPEG, including measurement data, on memory card. Built-in RAM for burst recording
Image storage mode	IR / visual images; simultaneous storage of IR and visual images Visual image is automatically associated with corresponding IR image
Periodic image storage	Every 10 seconds up to 24 hours
Panorama	For creating panorama images in FLIR Reporter Building software
Image annotations	
Voice	60 seconds stored with the image
Text	Predefined text or free text from PDA (via IrDA) stored with the image
Image marker	4 on IR or visual image
GPS	Location data automatically added to every image from built-in GPS
Video recording and streaming	
Radiometric IR-video recording	Real-time to built-in RAM, transferable to memory card.
Non-radiometric IR-video recording	MPEG-4 to memory card
Non-radiometric IR-video streaming	MPEG-4 to PC using USB or WLAN (optional)
Digital camera	
Built-in digital camera	3.2 Mpixel, auto focus, and video lamp
Laser pointer	
Laser	Activated by dedicated button
Data communication interfaces	
Interfaces	USB-mini, USB-A, IrDA, composite video, headset connection
Power system	
Battery	Li Ion, 3 hours operating time
Charging system	In camera (AC adapter or 12 V from a vehicle) or 2-bay charger
Power management	Automatic shutdown and sleep mode (user selectable)
Environmental data	
Operating temperature range	−15°C to +50°C
Storage temperature range	−40°C to +70°C
Humidity (operating and storage)	IEC 68-2-30/24 h 95% relative humidity +25°C to +40°C
Encapsulation	IP 54 (IEC 60529)
Bump	25 g (IEC 60068-2-29)
Vibration	2 g (IEC 60068-2-6)
Physical data	
Camera weight, incl. lens and battery	2.18 kg
Cameras size, incl. lens (L × W × H)	355 × 144 × 147 mm
Tripod mounting	UNC ¼"-20

Camera includes:
Hard transport case
Infrared camera with lens
Battery (2 ea., one inserted in camera, one outside camera)
Battery charger
Calibration certificate
FLIR QuickReport™ PC software CD-ROM
FireWire cable, 4/6
FireWire cable, 6/6
Headset
Lens cap (mounted on lens)
Lens cap (2 ea.)
Mains cable
Memory card-to-USB adapter
Memory card with adapter
Power supply
Printed Getting Started Guide
Shoulder strap
USB cable
User documentation CD-ROM
Video cable
Warranty extension card or Registration card

Supplies & Accessories
Close-up IR lens 0.5X, f = 75 mm (fits 24° IR lens) for ThermaCAM and FLIR 600 series
IR lens f = 76 mm, 12°, incl. case for FLIR 600 series
IR lens, f = 131 mm, 7°, incl. case for FLIR 600 series
IR lens f = 19 mm, 45°, incl. case for FLIR 600 series
IR lens f = 38 mm, 24°, incl. case for FLIR 600 series
Macro lens 1x (25 um) with case
High temperature option +2000°C
High temperature option +1500°C
Battery
Battery charger, incl. power supply and cable
Battery charger, incl. power supply and cable
Battery charger, incl. power supply and cable
Battery charger, incl. power supply with multi plugs
Power supply, incl. multi plugs
SD memory card, 1 GB
Adapter, SD memory card to USB
Memory card micro-SD with adapters
USB cable Std A <-> Mini-B, 2 m
FireWire cable 6/6, 2.0 m
FireWire cable 4/6, 2.0 m
Video cable, RCA <-> RCA, 2.0 m
Cigarette lighter adapter kit, 12 VDC, 1.2 m
Hard transport case for FLIR B/P/SC640
Headset, 3.5 mm plug
Remote Control Unit
FLIR Reporter Ver. 8.3 Professional (Sec. device)
FLIR Reporter Ver. 8.3 Professional
FLIR Reporter Ver. 8.3 Standard (Sec. device)
FLIR Reporter Ver. 8.3 Standard
FLIR BuildIR
FLIR Reporter Ver. 8.5 Standard
FLIR Reporter Ver. 8.5 Professional
Cover Visual Camera mkII

FLIR Reporter

FLIR Reporter software -
powerful yet easy-to-use tool to generate comprehensive and professional infrared inspection reports.

LASER RADIATION
DO NOT STARE INTO BEAM
CLASS 2 LASER PRODUCT

WAVELENGTH: 635 nm MAX. OUTPUT POWER: 1 mW
THIS PRODUCT COMPLIES WITH 21 CFR 1040.10 AND
1040.11 EXCEPT FOR DEVIATIONS PURSUANT TO
LASER NOTICE NO. 50, DATED JULY 26TH, 2001.

Asia Pacific Headquarter
Hong Kong
FLIR Systems Co Ltd.
Room 1613 – 16, Tower 2 Grand Central Plaza
138 Shatin Rural Committee Road, N.T, Hong Kong
Tel: +852 2792 8955   Fax: +852 2792 8952
Email: flir@flir.com.hk   Web: www.flir.com/thg

◆FLIR®

APPENDIX C: TABLE OF RESIDENTIAL BUILDING MAPPING FOR SOURCES OF HEAT LOSS
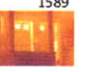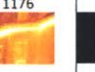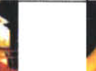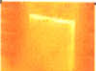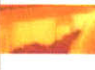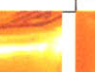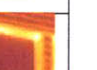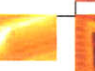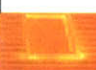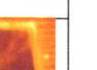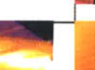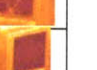
Image #	Window Frame/Casing	Window Surface	Window Crack	Basement	Door Crack	Corner	Chimney	Roof Ridge	Soffit	Well insulated window
	1637	1555	1444	1176	1589	1483	1616	1200	1176	1604
Example										
1155										
1164										
1170										
1176										
1182										
1188										
1194										
1200										
1204										
1210										
1216										
1220										
1229										
1235										

Image #	Window Frame/Casing	Window Surface	Window Crack	Basement	Door Crack	Corner	Chimney	Roof Ridge	Soffit	Well insulated window
1241										
1247										
1255										
1263										
1267										
1273										
1277										
1286										
1292										
1298										
1307										
1313										
1317										
1344										
1350										

Image #	Window Frame/Casing	Window Surface	Window Crack	Basement	Door Crack	Corner	Chimney	Roof Ridge	Soffit	Well insulated window
1356										
1362										
1368										
1383										
1389										
1403										
1417										
1425										
1431										
1438										
1444										
1450										
1456										
1471										
1477										

Image #	Window Frame/Casing	Window Surface	Window Crack	Basement	Door Crack	Corner	Chimney	Roof Ridge	Soffit	Well insulated window
1483										
1489										
1495										
1528										
1537										
1546										
1555										
1559										
1568										
1589										
1595										
1616										
1625										
1631										
1652										

Image #	Window Frame/Casing	Window Surface	Window Crack	Basement	Door Crack	Corner	Chimney	Roof Ridge	Soffit	Well insulated window
1661										
1670										
1679										
1688										
1697										
1706										
1715										
1724										
1733										
1751										
1763										
1784										
2018										
2036										
2048										

Image #	Window Frame/Casing	Window Surface	Window Crack	Basement	Door Crack	Corner	Chimney	Roof Ridge	Soffit	Well insulated window
2057										
2066										
2075										
1990										
2307										
2319										
2331										
2343										
2364										
2420										
2448										
2460										
2468										
2476										
2502										

Image #	Window Frame/Casing	Window Surface	Window Crack	Basement	Door Crack	Corner	Chimney	Roof Ridge	Soffit	Well insulated window
2538										
2601										
2631										
2661										
2693										
2758										
2809										
2930										
2947										
2968										
2994										
3003										
3012										
3028										
3040										

Image #	Window Frame/Casing	Window Surface	Window Crack	Basement	Door Crack	Corner	Chimney	Roof Ridge	Soffit	Well insulated window
3056										
3094										
3115										
3130										
3139										
3151										
3169										
3194										
3260										
3288										
3316										
3550										
3565										
3573										
4028										

Image #	Window Frame/Casing	Window Surface	Window Crack	Basement	Door Crack	Corner	Chimney	Roof Ridge	Soffit	Well insulated window
3616										
3674										
3729										
4188										
4360										
4366										
4377										
4380										
4386										
4392										
4400										
4408										
4428										
4710										
4949										
5056										
TOTAL	39	125	124	63	25	31	70	25	98	111
100%	135	135	135	135	135	135	94	135	135	135
%	29%	93%	92%	47%	19%	23%	74%	19%	73%	82%